

# On the Reverse-Link Capacity of CDMA Macrodiversity Systems

Halim Yankömeroğlu

Department of Systems & Computer Engineering — Carleton University, Ottawa  
halim@sce.carleton.ca

**Abstract** — The upper bound of the reverse-link capacity of CDMA macrodiversity systems is given in [1]. It is shown in that study that, under limiting conditions, there is a linear increase in capacity with an increasing number of antenna elements, and that the capacity becomes independent of the locations of the wireless users. One main condition in achieving this bound and the corresponding independence statement is the requirement for an infinitely large spread spectrum bandwidth. In this study, we present intermediate results that will help in determining the capacity loss incurred in a real system due to finite bandwidth, and also in analyzing the effects of user and antenna locations on capacity.

## 1 Introduction

We consider a macrodiversity system with  $L$  antenna elements (AE's), where the outputs of the AE's are conveyed to a central station (CS) for joint decoding and combining, through the use of a Rake receiver and a maximal ratio combiner (MRC). We remark that the reverse-link of a CDMA multi-antenna system is inherently different than its forward link, since in the reverse-link, diversity can be achieved without injecting extra energy into the system.

We consider a macrodiversity system where the multipath fading is averaged out. This can be attained through the employment of other forms of diversity techniques in conjunction with the macrodiversity type.

It is interesting to point out that such a macrodiversity system is fundamentally different from a set of collocated AE's arranged in a microdiversity manner, which is effective mainly for mitigating against fast fading. The microdiversity scheme yields, in the limit, a wireless channel that does not fade. A significant diversity benefit is achieved against fast fading with a small number of AE's, but the performance returns diminish fairly quickly with increasing number of AE's.

It is important to note that in the case of a set of collocated antennas, the mean values of the interference components at each diversity branch are the same. In other words, after averaging out the multipath fading, the interference components at each diversity branch become identical. Therefore, once the multipath fading is mit-

igated against, there is no further gain against the interference, no matter how many AE's are employed; this is due to the fact that the entire set of collocated AE's is equivalent to a single AE in a macrodiversity scheme where multipath fading is averaged out.

In a macrodiversity system, on the other hand, the mean interference levels at the diversity branches will, in general, be different, and for certain system parameters (which we will discuss later), these quantities will be uncorrelated. In this case, there is a potential for more and more diversity gain, simply by deploying more AE's. Hanly [1] has shown that such a network of antennas, in the limiting conditions, yields a linear increase in the system capacity which also becomes independent of user locations.<sup>1</sup> The limiting conditions in obtaining the upper bound for capacity ([1]) are as follows: a) all base stations (AE's) in the service region are involved in the joint processing, b) there is no constraint on the maximum transmit power level of the wireless terminals, and c) the spread spectrum bandwidth approaches infinity.

The key condition in achieving the capacity upper bound of such a macrodiversity system is that the (averaged out) interference components at the branches of the combiner should be uncorrelated. Otherwise, the output SIR of the MRC will be less than the sum of the branch SIR's. In the

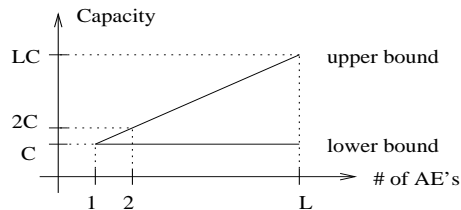


Figure 1: The upper and lower bounds for the reverse-link capacity of a CDMA macrodiversity system.

limit, if these quantities become identical, the combiner will reduce to that which has only one effective branch; thus no diversity gain will be attained. This situation corresponds to the lower bound for the capacity. The upper and lower bounds for the capacity are shown in Fig. 1.

In this study we will present some intermediate results

<sup>1</sup>Less general results in the same line are obtained in [2].

that may help in determining the impact of relaxing the strongest of the above mentioned limiting conditions (infinite bandwidth) on system capacity. The consequence of a finite spread spectrum bandwidth is the possibility of correlated interference which degrades the performance.

## 2 Spatial Correlated Interference Analysis for $L=2, K=2$ [3]

The correlated interference analysis for the simplest non-trivial macrodiversity system which has 2 AE's and 2 users ( $L=2, K=2$ ) is presented in [3]. The total propagation time from user  $i$  ( $w_i$ ) to the CS through AE  $j$ ,  $t_{ij,t}$ , is equal to the sum of the propagation times in the air,  $t_{ij}$ , and in the cable,  $t_{j,c}$ :  $t_{ij,t} = t_{ij} + t_{j,c}$ , where  $i \in \{1, 2\}, j \in \{I, II\}$ .

The baseband transmitters and receivers are illustrated in Fig. 2. Also, the spreading code and the related as-

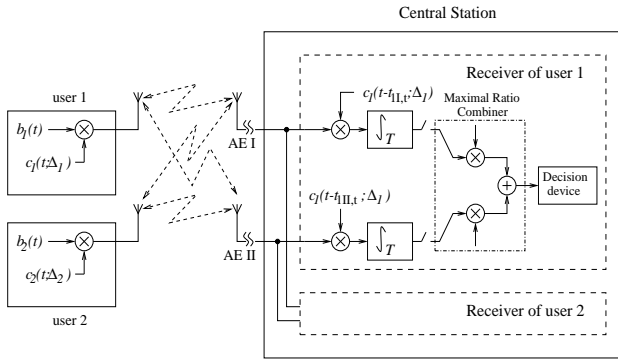


Figure 2: The baseband transmitters and receivers.

sumptions are depicted in Fig. 3.  $c_i(t)$  is the spreading

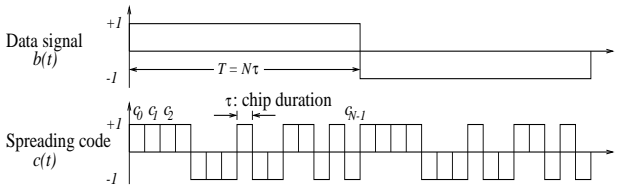


Figure 3: The data signal,  $b(t)$ , and spreading code,  $c(t)$ .

code for  $w_i$  and  $\Delta_i$  is the corresponding (normalized) code phase.  $\Delta_i$  is represented in terms of  $\tau$  (chip duration); i.e.,  $c_i(t - t_{ij,t}; \Delta_i) = c_i(t - t_{ij,t} - \Delta_i\tau)$ , where  $i \in \{1, 2\}$  and  $j \in \{I, II\}$ . It is assumed that the spreading codes are formed from i.i.d. Bernoulli random variables. The background noise is omitted in this analysis.

Let  $n_{1I}$  and  $n_{1II}$  be the mean interference components (after despreading) at the branches of the MRC of  $w_1$ , corresponding to AE's  $I$  and  $II$ , respectively:

$$n_{1j} = \langle c_1(t - t_{1j,t}; \Delta_1) c_2(t - t_{2j,t}; \Delta_2) \rangle, \quad (1)$$

where  $\langle \cdot \rangle$  denotes the inner product (refer to Fig. 3) and

$j \in \{I, II\}$ . Likewise,  $s_{1I}$  and  $s_{2II}$  are the corresponding mean signal components at the combiner branches.

We are interested in evaluating the correlation coefficient of the random variables  $n_{1I}$  and  $n_{1II}$ , denoted by  $\rho$ :

$$\rho = \frac{\mathbf{E}(n_{1I} n_{1II}) - \mathbf{E}(n_{1I})\mathbf{E}(n_{1II})}{\sqrt{\mathbf{E}(n_{1I}^2) - \mathbf{E}^2(n_{1I})} \sqrt{\mathbf{E}(n_{1II}^2) - \mathbf{E}^2(n_{1II})}}, \quad (2)$$

where  $\mathbf{E}(\cdot)$  denotes the expectation operator.

It is shown in [3] that for uncorrelated interference, the following conditions in terms of  $t_{12I}$  and  $t_{12II}$  should hold:

$$\begin{aligned} t_{12I} = n\tau &\longrightarrow \\ \begin{cases} \rho = 0, & \text{for } t_{12II} \leq (n-1)\tau \text{ and } t_{12II} \geq (n+1)\tau \\ 0 < \rho \leq 1, & \text{for } (n-1)\tau < t_{12II} < (n+1)\tau, \end{cases} \\ n\tau < t_{12I} < (n+1)\tau &\longrightarrow \\ \begin{cases} \rho = 0, & \text{for } t_{12II} \leq (n-1)\tau \text{ and } t_{12II} \geq (n+2)\tau \\ 0 < \rho \leq 1, & \text{for } (n-1)\tau < t_{12II} < (n+2)\tau, \end{cases} \end{aligned} \quad (3)$$

where  $n$  is an integer, and

$$t_{12j} = t_{1j,t} - t_{2j,t} = (t_{1j} + t_{j,c}) - (t_{2j} + t_{j,c}) = t_{1j} - t_{2j}, \quad (4)$$

where  $j \in \{I, II\}$ . It is observed from (4) that  $t_{12I}$  and  $t_{12II}$  depend only on the propagation delays in the air.

Since the propagation time depends on the distance, we can obtain similar conditions in distance domain. For a given set of AE and  $w_1$  locations, we can obtain a ‘‘caution zone’’ for  $w_1$ . The interference resulting from a user in

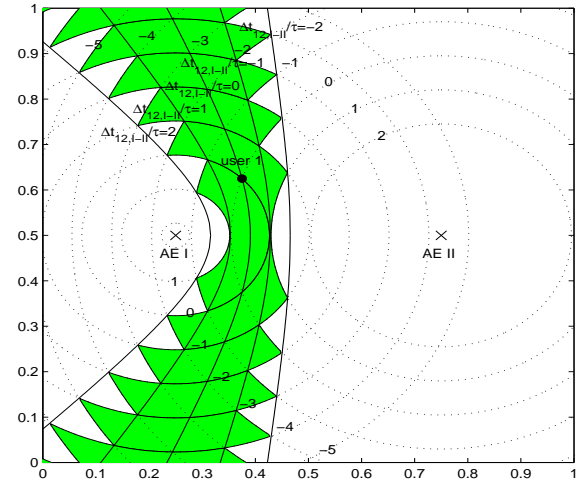


Figure 4: The  $\Delta t_{12,I-II}/\tau = -2, -1, \dots, 1$  lines along with the caution zone for  $w_1$ , for the case of synchronous users ( $\Delta_1 = \Delta_2$ ), with  $s = 400$  and  $R_c = 10$  Mcps.

this zone, at the  $I$ st branch of  $w_1$ 's combiner at the CS, will be correlated with the corresponding interference at the  $II$ nd branch.

The boundaries of a caution zone can be approximated by a pair of hyperbolas. In order to demonstrate this we

define the differential delay,  $\Delta t_{12,I-II}$ , as

$$\Delta t_{12,I-II} = t_{12I} - t_{12II} = (t_{1I} - t_{2I}) - (t_{1II} - t_{2II}), \quad (5)$$

which can be rewritten as  $\Delta t_{12,I-II} = (t_{1I} - t_{1II}) - (t_{2I} - t_{2II})$ . It is shown in [3] that

$$|\Delta t_{12,I-II}|/\tau = 0 \longrightarrow \rho = 1, \quad (6)$$

$$|\Delta t_{12,I-II}|/\tau \geq 2 \longrightarrow \rho = 0. \quad (7)$$

$$1 \leq |\Delta t_{12,I-II}|/\tau < 2 \longrightarrow 0 \leq \rho \leq 0.5. \quad (8)$$

We choose the following pair of hyperbolas for the approximation of the caution zones:

$$|\Delta t_{12,I-II}|/\tau > 1. \quad (9)$$

Fig. 4 shows the  $\Delta t_{12,I-II}/\tau = -2, -1, \dots, 2$  lines along with the actual caution zone (shaded region), for a system where the service region is a square with side length  $s = 400$  meters and chip rate  $R_c = 10$  Mcps. According to (9), the caution zone in Fig. 4 can be approximated by the area between the  $\Delta t_{12,I-II}/\tau = -1$  and 1 lines. We know from (8) that  $\rho$  is less than 0.5 in the shaded regions outside the approximated caution zones, therefore, the performance degradation introduced by such an approximation is expected to be insignificant.

It can be shown that  $\Delta t_{12,I-II}/\tau$  is proportional to the product  $sR_c$ , which turns out to be the most important system parameter. It is also noticed that for a certain value of the product  $sR_c$ , the actual values of  $s$  and  $R_c$  do not matter. Hence, as long as the correlation analysis is concerned, a system with  $s = 400$  and  $R_c = 10$  Mcps is equivalent to the one with  $s = 1000$  and  $R_c = 4$  Mcps.

For a large  $sR_c$  value, the hyperbolic grid will be denser; since the approximate caution zone is the area between the hyperbolas -1 and 1, this area will be smaller. Therefore, it is desirable to have a large  $sR_c$  value. The density and orientation of the hyperbolic grid also depend on the AE locations in the service area. For a given  $sR_c$  value, the density of the hyperbolic grid will increase with increasing distance between the AE's. Therefore, to minimize the caution zone (and thus, the correlation effect), AE's must be placed as far apart as possible — an intuitively satisfying result.

Also, if  $s$  is small, the AE's will inevitably become close to each other, increasing the caution zone. In the limit, when the AE's become collocated, the entire service region becomes the caution zone yielding no macrodiversity gain (lower bound). Finally, if the bandwidth is very large, then even the closely spaced AE's will not yield a large caution zone; therefore, more AE's can be placed for macrodiversity gain. It is worth noting that even for a large  $sR_c$  product (small caution zones), if the two users are close to each other, there is still a high likelihood of correlated interference affect.

These results are in agreement with those presented in [1]: in the limiting case of infinite bandwidth ( $R_c \rightarrow \infty$ )

the caution zone reduces to a line, and the probability of  $w_2$  being on this line approaches zero.

### 3 Correlation Analysis for $L = 2$ with Many Users

The analysis presented in the last section ([3]) corresponds to the simplest nontrivial macrodiversity system of  $L = 2$  AE's with  $K = 2$  users. In this section, we will extend our analysis to the more general case of  $L = 2$  with many users.

In a system with  $K$  users, for each  $w_i$ , we determine whether the remaining  $K-1$  users are in the caution zone for  $w_i$ . By this way, we construct a  $K \times K$  correlation

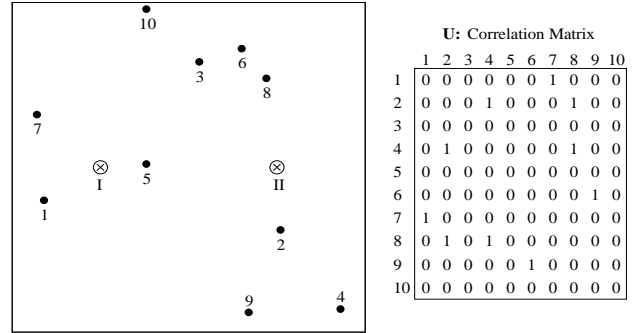


Figure 5: A system with  $L = 2$  and  $K = 10$ , and the corresponding correlation matrix,  $\mathbf{U}$ , for  $s = 400$  meters and  $R_c = 10$  Mcps.

matrix,  $\mathbf{U} = \{u_{ij}\}$  such that

$$u_{ij} = \begin{cases} 0, & \text{if } w_j \text{ is not in the caution zone for } w_i, \\ 1, & \text{if } w_j \text{ is in the caution zone for } w_i. \end{cases} \quad (10)$$

We note that  $u_{ii} = 0$ ,  $i = 1, 2, \dots, K$ , since a user does not create interference to itself. Also, it can be shown that if  $w_j$  is in the caution zone for  $w_i$ , then  $w_i$  must be in the caution zone for  $w_j$ . It can further be shown that if  $w_j$  is in the caution zone for  $w_i$ , and  $w_k$  is in the caution zone for  $w_j$ , then this does not necessarily mean that  $w_k$  will be in the caution zone for  $w_i$ . The conclusion from the above two sentences, in mathematical terms, is that  $\mathbf{U}$  is a symmetric non-transitive matrix.

In Fig. 5, a system with  $L = 2$  and  $K = 10$  is illustrated and the corresponding  $\mathbf{U}$  matrix is given ( $s = 400$  m and  $R_c = 10$  Mcps). In Fig. 5, the caution zones are not drawn. But, if we were to draw the caution zone for user 8, for instance, then  $w_2$  and  $w_4$  would be in that caution zone. Consequently,  $u_{82} = 1$ ,  $u_{84} = 1$ , and all the other entries in the 8th row of the  $\mathbf{U}$  matrix are 0's.

In the worst case, all of the  $K-1$  entries in a row of  $\mathbf{U}$  will be 1's, and in the best case, all of those entries will be 0's. Based on this observation, we define a quantity which we call percent correlation,  $\phi$ , as follows

$$\phi_i = \frac{\sum_{j=1}^K u_{ij}}{K-1} \times 100, \quad i = 1, 2, \dots, K. \quad (11)$$

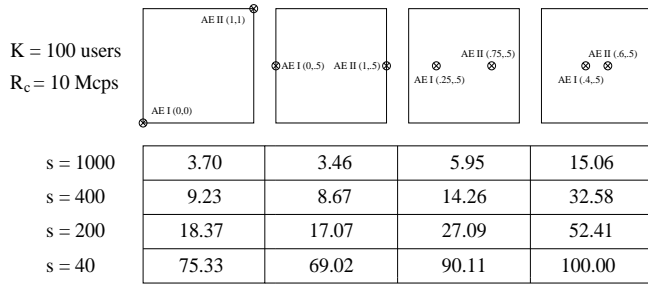


Figure 6: The average percent correlation,  $\bar{\phi}$ , values for various combinations of AE locations, and  $s$  and  $R_c$  values, in systems with  $L=2$  and  $K=100$ .

It is worth noting that  $\phi$  is not equal to the correlation coefficient.

The percent correlation for a user will depend on that particular user's location in the system, as well as the AE locations, and  $s$  and  $R_c$  values. Simulations have been run to obtain the  $\phi$  values for various combinations of these system parameters. For each such combination, 100 systems (each with  $L=2$  and  $K=100$ ) are randomly (uniform user distribution) generated; consequently, a total of 10,000  $\phi$  values are collected. The arithmetic means of these values,  $\bar{\phi}$ , for various combinations of the system parameters, are given in Fig. 6.

#### 4 Correlation Analysis for Many AE's with Many Users

In this section, we extend our analysis to the most general case of  $L$  AE's with  $K$  users.

In this case, for each user, a total of  $L(L-1)/2$  caution zones exist, each of which corresponds to a particular AE pair. Therefore, the  $\mathbf{U}$  matrix is composed of  $L(L-1)/2$  submatrices (one for each antenna pair), with sizes  $K \times K$ . Consequently, the correlation matrix,  $\mathbf{U}$ , is 3-dimensional

all of the remaining  $K-1$  users are in all of the  $L(L-1)/2$  caution zones for  $w_i$ . Obviously, this is an event with a very low likelihood! Such a situation will yield  $(K-1)[L(L-1)/2]$  1's in the 2-dimensional  $i$ th row of the  $\mathbf{U}$  matrix. Based on this observation, we define the percent correlation,  $\phi$ , as

$$\phi_i = \frac{\sum_{k=1}^{L(L-1)/2} \sum_{j=1}^K u_{ijk}}{(K-1)L(L-1)/2} \times 100, \quad i = 1, 2, \dots, K. \quad (12)$$

The size of the simulations grows rapidly due to the  $L(L-1)/2$  factor. Therefore, we considered only  $L=4$  and  $K=100$  case with  $s=400$  m and  $R_c=10$  Mcps. The AE's are located at  $(100,300)$ ,  $(300,300)$ ,  $(100,100)$  and  $(300,100)$ . Similar to the simulations in the previous section, 100 systems are randomly (uniform user distribution) generated, and thus, a total of 10,000  $\phi$  values are collected. The average percent correlation,  $\bar{\phi}$ , is found to be 12.75.

#### 5 Concluding Remarks

We observed that the size of the caution zone (and thus, the likelihood of having a reduction in capacity due to the correlated interference effects) depends on the size of the service region, chip rate, and the locations of the wireless users and the AE's. Increasing the spread spectrum bandwidth, and placing the AE's as far as possible from each other results in a reduction in the correlation between the interference components at the combiner branches. This implies that for reasonably high chip rates (wideband-CDMA) and for service regions that are not very small, the capacity penalty incurred (in comparison to the potential linear gain) would be low if the number of AE's is not very high. Further investigation is required to quantify these conclusions. Finally, it is worth noting that, to the best of the author's knowledge, there exists almost no literature on the spatial correlation analysis in CDMA macrodiversity systems.

#### Acknowledgments

I would like to thank Professor E. S. Sousa (University of Toronto) for his valuable contributions to this study.

#### References

- [1] S. V. Hanly, "Capacity and power control in spread spectrum macrodiversity radio networks", *IEEE Trans. Commun.*, v. 44, no. 2, pp. 247-256, Feb. 1996.
- [2] H. Yanikomeroglu and E. S. Sousa, "CDMA sectorized distributed antenna system", *Proc. Int. Symp. Spread Spectrum Technology and Applications (ISSSTA'98)*, pp. 792-797, September 1998, Sun City, South Africa.
- [3] H. Yanikomeroglu and Elvino S. Sousa, "Correlated interference analysis in CDMA multi-antenna systems", *Proc. IEEE Int. Conf. Commun. (ICC'99)*, 6-10 June 1999, Vancouver, BC, Canada.

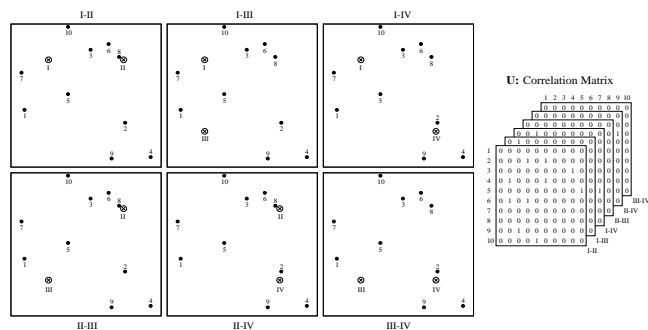


Figure 7: A system with  $L=4$  and  $K=10$ , and the corresponding correlation matrix,  $\mathbf{U}$ , for  $s=400$  m and  $R_c=10$  Mcps.

with size  $K \times K \times [L(L-1)/2]$ . Such a system, for the case of  $L=4$  and  $K=10$ , is illustrated in Fig. 7.

For a  $w_i$ , the most disadvantageous situation will occur if